Dynamic strain-induced giant electroresistance and erasing effect in ultrathin ferroelectric tunnel-junction memory

Hei-Man Yau,[1] Zhongnan Xi,[2] Xinxin Chen,[1] Zheng Wen,[1,2] Ge Wu,[3] and Ji-Yan Dai[1,*]

[1]*Department of Applied Physics, The Hong Kong Polytechnic University, Hung Hom, Kowloon, Hong Kong*

[2]*College of Physics, Qingdao University, Qingdao 266071, China*

[3]*Department of Mechanical and Biomedical Engineering, City University of Hong Kong, Tat Chee Avenue, Kowloon, Hong Kong*

(Received 24 November 2016; revised manuscript received 31 March 2017; published 12 June 2017)

Strain engineering plays a critical role in ferroelectric memories. In this work, we demonstrate dynamic strain modulation on tunneling electroresistance in a four-unit-cell ultrathin $BaTiO_3$ metal/ferroelectric/semiconductor tunnel junction by applying mechanical stress to the device. With an extra compressive strain induced by mechanical stress, which is dynamically applied beyond the lattice mismatch between the $BaTiO_3$ layer and the Nb : $SrTiO_3$ substrate, the ON/OFF current ratio increases significantly up to a record high value of 10^7, whereas a mechanical erasing effect can be observed when a tensile stress is applied. This dynamic strain engineering gives rise to an efficient modulation of ON/OFF ratio due to the variation of $BaTiO_3$ polarization. This result sheds light on the mechanism of electroresistance in the ferroelectric tunnel junctions by providing direct evidence for polarization-induced resistive switching, and also provides another stimulus for memory state operation.

DOI: 10.1103/PhysRevB.95.214304

I. INTRODUCTION

Resistive switching of oxides has attracted a great deal of attention with regard to its potential application for nonvolatile memories in data storage. The nonvolatile switching has been divided into several types, such as resistive random-access memory (ReRAM), magnetoresistive RAM (MRAM), phase-change memory (PCM), and so on, but a general characteristic which is common for all types is their two different resistance states, which can be switched from one to another by applying appropriate electric stimulus [1,2]. Most recently, direct evidence of a switching mechanism has been observed. For example, Yang *et al.* [3] and Liu *et al.* [4] reported real-time observation on the formation/rupture of conducting filaments in ReRAMs, while Yang *et al.* [5] observed the existence of oxygen vacancies involved in resistance switching by using *in situ* transmission electron microscopy. However, for a new type of emerging memories–ferroelectric tunnel junction (FTJ) type of resistive memory, the experimental evidence of polarization-induced resistive switching is mainly the correlation between resistive switching and ferroelectric switching [6–8]. However, the conductive filaments might be formed as a result of the migration of oxygen vacancies under external electric stimuli, which may also result in the resistance change, in parallel with the polarization reversal. Therefore, a direct evidence to illustrate the role of ferroelectric polarization in resistive switching of the FTJ devices is desirable to rule out other factors, such as oxygen vacancies and interfacial effects.

By utilizing reversible polarization of ferroelectric materials such as $Pb(Zr,Ti)O_3$ and $BaTiO_3$ (BTO) [9–13], ferroelectric oxide–based memory devices have shown promising properties of long write/read cycle endurance and lifetime retention, as well as low power consumption. Tunnel junctions utilizing the ultrathin ferroelectrics as the barriers, i.e., the so-called FTJs, is one of the prospective ways to achieve giant electroresistance [6,14,15]. Researchers have reported a variety of ways to improve the magnitude and stability of the switchable ferroelectric-induced electroresistance in these junctions. Among them, in-plane strain has shown its significance due to the fact that ferroelectric polarization and domain switching are strongly coupled with strain, especially in epitaxial ferroelectric thin films. For instance, compressively strained BTO exhibits a shift to higher ferroelectric-paraelectric transition temperatures and hence an enhanced spontaneous polarization [16–18]. Due to the lattice mismatch, strain applied to the perovskite may change the tetragonality, i.e., c/a. Then, atomic displacements associated with tetragonality tend to change the ferroelectric polarization [19,20]. Meanwhile, several reports have simulated the properties of ferroelectric films, including phase diagrams with tensile and compressive in-plane strains [21]. Their influence on ferroelectric behavior and distortions in relation to strain and remnant polarization have also been discussed [22–25]. Recently, a report of De Luca and co-workers using a combination of scanning transmission electron microscopy and optical second-harmonic generation has determined the relationship between strain and domain wall structure [26]. Strain-dependent polarization also shows the influences of the domain walls and strain-controlled charges of domain on velocity [27]. However, previous experimental evidences, by considering different thicknesses or substrates with different lattice constants [16,21,28], cannot simply present the influence of strain on the junction. By reason of the different thin film growth conditions and substrates, their results consist of more than one variation, such as different densities of oxygen vacancies and space charges and interdiffusion. Besides, the strain induced by using piezoelectric or magnetostrictive materials [27,29] is relatively small [$\varepsilon = 0.13\%$ for PMNPT ($0.72PbMg_{1/3}Nb_{2/3}O_3 - 0.28PbTiO_3$)]. It also may not be fully transferred to the thin film if it is connected by glues or the thin film is difficult to grow because of a large misfit of the lattice parameters. Therefore, a direct evidence and dynamic way to illustrate the role of ferroelectric polarization in resistive switching by ruling out other factors is still desirable.

*jiyan.dai@polyu.edu.hk

2469-9950/2017/95(21)/214304(7)

©2017 American Physical Society

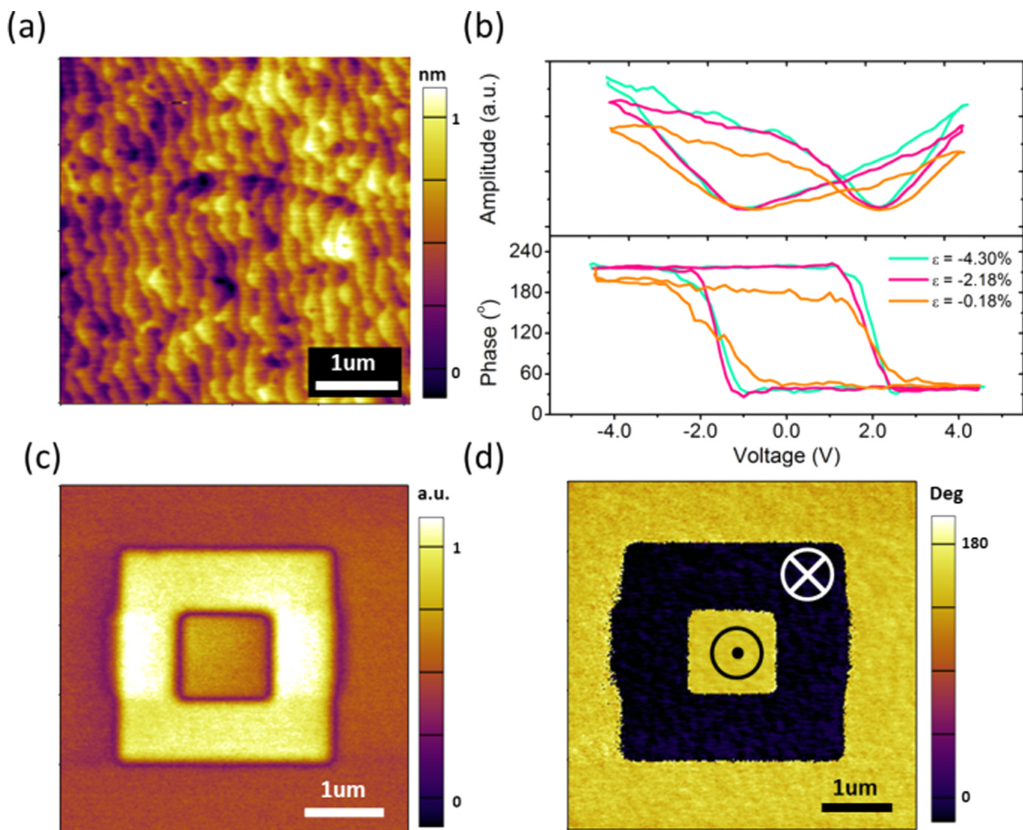

FIG. 1. (a) Morphology of the 4-u.c. BTO surface on NSTO substrate; (b) PFM amplitude and phase hysteresis loops as a function of strain in the cases of $\varepsilon = -4.30\%, -2.18\%$, and -0.18%; (c) PFM out-of-plane amplitude; and (d) phase images recorded after writing an area of $3.0 \times 3.0\,\mu\text{m}^2$ with -4.5 V and then the central square with $+4.5$ V using a biased conductive tip for the epitaxial BTO thin films.

In this article, we introduce a dynamic mechanical strain modulation to the tetragonality (and thus the spontaneous polarization) of ultrathin BTO film by adding an additional strain to sample through our specially designed bending device. In the meantime, electroresistance of the FTJ is measured. Dissimilar to the compressive ultrathin film BTO reported by Wen *et al.* [10], where the ON/OFF ratio is above 10^4 at room temperature with lattice mismatch to a semiconducting bottom electrode Nb-doped $SrTiO_3$ (NSTO), our external stress can increase or decrease the strain in the film beyond its original state. Hence, the ON/OFF ratio of the tunnel-junction memory state may be further increased or mechanically erased. Through this strain modulation, a critical role of ferroelectricity to the resistive switching can be clearly demonstrated. Also, compared to the strain induced by lattice mismatch, which is a method generally being used for tuning ferroelectricity of thin films, a dynamic strain tuning is an elaborate approach to study the strain engineering effect within the same system and also provide another stimulus for memory state operation.

II. FERROELECTRICITY OF BTO

A four-unit-cell (u.c.)-thick BTO ultrathin film was deposited epitaxially on a (001)-oriented single-crystalline NSTO substrate using a KrF excimer laser ($\lambda = 248$ nm) by pulsed-laser deposition. With $2.5\,\text{J}\,\text{cm}^{-2}$ laser energy density in a typical layer-by-layer growth mode, as shown in Fig. 1(a), details of single-crystal growth are described elsewhere [10,30]. The BTO/NSTO heterostructure exhibits an atomically flat surface with step of about 0.4 nm heights, indicating that these steps are single-unit-cell high and also maintain the step terrace of the substrate. It is known that BTO has relatively larger lattice constants ($a = 3.992\,\text{Å}, c = 4.036\,\text{Å}$) compared to those of NSTO ($a = c = 3.905\,\text{Å}$), so the lattice mismatch ($\varepsilon = -2.18\%$) ensures that BTO is under a compressive strain with the c axis along the film normal direction. The c/a ratio should be larger than bulk due to the compressive strain at room temperature [31,32] and therefore its ferroelectric polarization is enhanced [7,10,33]. The piezoresponse force microscopy (PFM) with Pt/Ti-coated silicon cantilevers was used to demonstrate its polarization switching and domain structure. Figures 1(b)–1(d) display the out-of-plane PFM amplitude and phase hysteresis loop, as well as the images of the BTO film as a ferroelectric domain structure written on the BTO with ±4.5 V before applying any external stresses. The 180° phase contrast and the minimum amplitude in the boundary reveal the domain structure with antiparallel polarizations. With the support of previous work according to Strelcov *et al.*, these results confirmed the ferroelectric nature of the 4-u.c.-thick BTO film [30,34]. Followed by magnetron sputtering, Pt top electrodes of 30 μm diameter and 50 nm thickness using a shadow mask were deposited on the BTO/NSTO structure to form metal/ferroelectric/ semiconductor (MFS) structure FTJs.

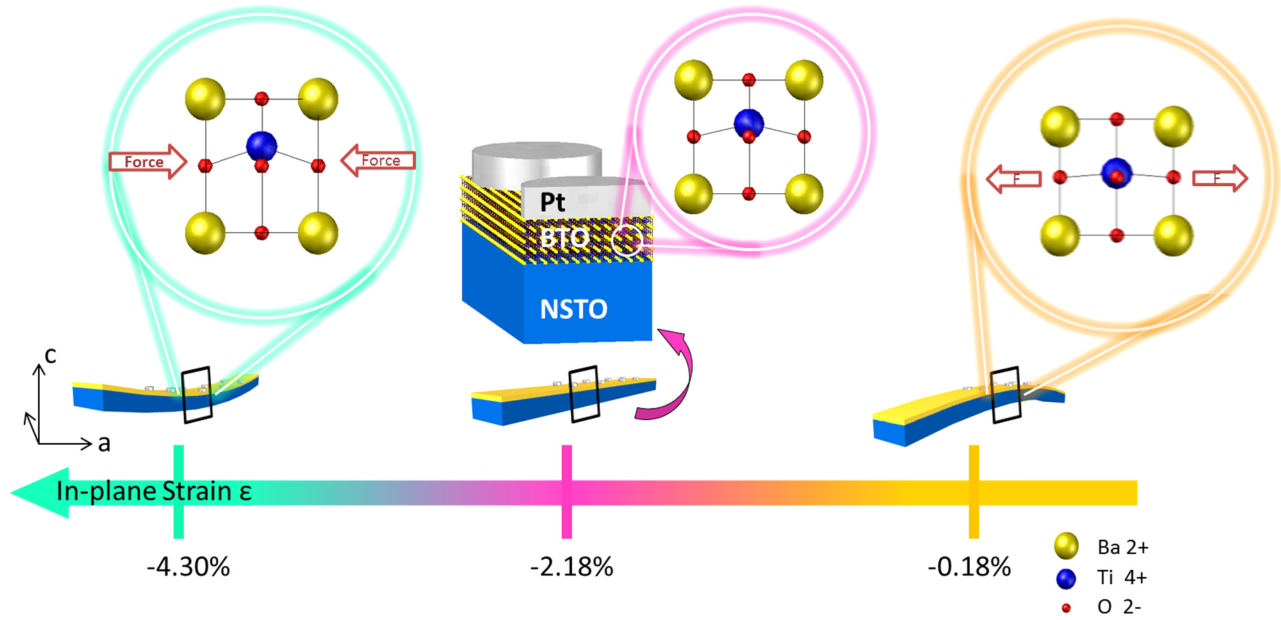

FIG. 2. Schematic description of the experiment showing strain of the junction induced by external stresses as a result of bending. The experimental setup for compressive and tensile stress application and a sketch of the corresponding BTO lattice structure of the junction in a compressive-stressed state ($\varepsilon = -4.30\%$), original state with strain induced by pure lattice mismatch ($\varepsilon = -2.18\%$), and a tensile-stressed state ($\varepsilon = -0.18\%$) are shown.

III. STRAIN MODULATION ON FTJ

Figure 2 schematically illustrates the experimental setup and the sample structure used in this work. A 0.5-mm-thick sample was cut into a size of 10 mm in length (L) and 2.5 mm in width (W), aiming to only consider the principal stress and strain in the system. As the bar length is much greater than the thickness, shear stress and strain can be neglected [35]. The sample is then bent into u-shaped or n-shaped form with a specially designed tool. However, to simplify, we assume that there is no strain gradient in the Pt/BTO/NSTO FTJ (the bending is very small, as illustrated in Supplemental Material, Fig. S1 [36]), but only in-plane strains are present. The resulting strain is obtained by summing up two parts. The first part is the strain induced by lattice mismatch, and the second part is the strain calculated from the distance change ΔL in bending curvature for the BTO layer observed from an optical surface profiler. The resultant strains, thus in the form of tensile-stressed, nonstressed, and compressive-stressed, are $\varepsilon = -0.18\%, -2.18\%$, and -4.30%, respectively. The corresponding crystal structures of the BTO film under these states are displayed in Fig. 2.

Based on the assumption that BTO would not be strain relaxed within the thickness of 4 u.c., a large compressive strain results in the increase of tetragonality with polarization in the c axis [17]. While under an induced strain perpendicular to the out-of-plane polarization, the magnitude of polarization along the c axis should be changed as the c/a ratio varies corresponding to the substrate lattice. The shift in the peak of substrate in x-ray diffraction in the Supplemental Material Fig. S2 shows the elongation along the c axis when it is bent into a u-shape. It is interesting to notice in Fig. 1(b) that the magnitude of the hysteretic amplitude loop increases for $\varepsilon = -4.30\%$, whereas it decreases for $\varepsilon = -0.18\%$. This difference can be attributed to the different ferroelectric properties induced by different strain conditions. This is in good agreement with reported PFM observations on the fully strained BTO ultrathin films on $SrTiO_3$ (STO), $DyScO_3$ (DSO), and $GdScO_3$ (GSO) substrates, respectively, using $SrRuO_3$ (SRO) as the bottom electrode [28].

For the electrical measurements, resistance-voltage (R-V) curves showed in Fig. 3 confirm the nonvolatile resistance switching of the Pt/BTO/NSTO FTJ at room temperature. Pulsed-train writing voltages were used in the sequence illustrated with a step of 0.5 V, and the read voltage remained unchanged as $V_{\text{read}} = 0.2$ V [37]. The positive voltage pulse drives the BTO polarization pointing to NSTO electrode and sets the junction to the ON state. The Pt/BTO/NSTO is set to the OFF state by applying a negative pulse, which switches the polarization towards the Pt electrode. For the BTO layer with $\varepsilon = -2.18\%$, R-V measurement with an ON/OFF ratio above 10^4 is observed. It is obvious that the change from the OFF to the ON states is relatively sharper compared to that from the ON to the OFF states, suggesting the widening of the space charge region on the NSTO surface because of the increased voltage pointing from the NSTO semiconductor to the BTO layer.

By measuring 30 cycles of R-V hysteresis loops in different strain states, it turns out that the smaller compressive strain of the junction, the smaller its ON/OFF ratio. At $\varepsilon = -0.18\%$, the memory state tends to be erased. The significant decrease of the ON/OFF ratio is attributed to the polarization decrease due the release of the compressive strain. It has been reported in a simulation work that spontaneous polarization drops if in-plane tensile stress is applied to an epitaxial BTO thin film [16,17]. Under a tensile stress, the in-plane lattice expands perpendicular to the polarization direction, resulting in a decreased c/a ratio, so that the strength of polarization is

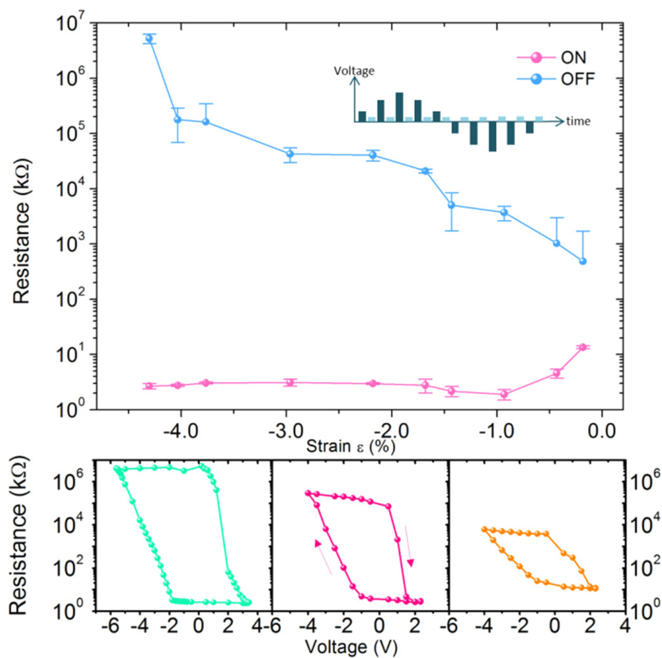

FIG. 3. Resistance variations with in-plane strains. ON and OFF states are recorded with different in-plane strain. Resistance hysteresis loops of FTJ at different strain states are measured using the write pulse voltage following a triangular profile between $+V$ and $-V$. Read pulses of 0.2 V were applied after each write pulse. The error bar is added under a calculation of standard deviation on the entire population which was measured from three junctions (ten cycles for one junction).

weaker than that of the original. Thus, the ON state resistance rises and the OFF state resistance drops, resulting in a degradation of the ON/OFF ratio with increasing tensile strain. Additionally, retention and endurance properties in Fig. S3 of the Supplemental Material [36] show the lifetime for the data as well as reproducibility, respectively. Although the repeatable cycles show the reproducibility in the two resistance states, compared to the strain state of $\varepsilon = -2.18\%$, the OFF state at $\varepsilon = -0.18\%$ decreases gradually, suggesting that smaller polarization also results in poor memory retention.

On the other hand, performance of the FTJ including ON/OFF ratio and retention is improved when external compressive strain is added to the junction from $\varepsilon = -2.18\%$ step-by-step. It is remarkable to see that the compressive strain induces an enhancement to the ON/OFF ratio. Importantly, it should be noticed that the actual strain is approximately equal to -4.30%, and under this situation, BTO is practicing a huge compressive strain. Therefore the tetragonality and ferroelectricity of the BTO film should be further enhanced due to the increase of the two Ti-O distances (along the c-oriented Ti-O chain) [20]. One can see that from $\varepsilon = -0.18\%$ to -4.30%, the ON state resistance changes only a little, but the resistance of the OFF state rises significantly when compressive strain increases. These results are in agreement with our prediction that when polarization becomes stronger, the depletion region at the NSTO surface becomes wider, resulting in a large increase of resistance. Consequently, the ratio of electroresistance is greatly enhanced. Besides, the increased compressive strain for $\varepsilon = -4.30\%$ results in good reproducibility and retention (Fig. S3).

Current-voltage (I-V) curves in Fig. 4(a) show the change of currents with different external strains. It can be seen that when the BTO junction is under tensile stress, i.e., from $\varepsilon = -4.30\%$ to -0.18%, the current in the ON state shifts to a smaller value while the current in the OFF state

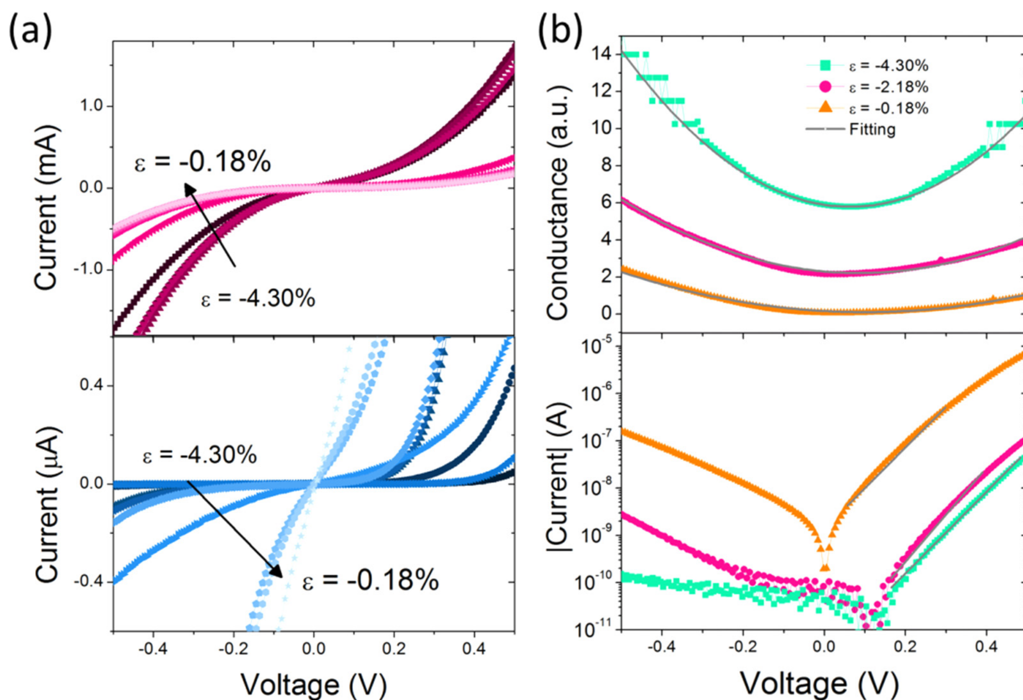

FIG. 4. I-V characteristics as a function of strain. (a) I-V curves recorded with different strains for the ON (top) and OFF (bottom) state. (b) Fitting by the direct tunneling model for the ON state (top) and the thermionic emission model for the OFF state (bottom).

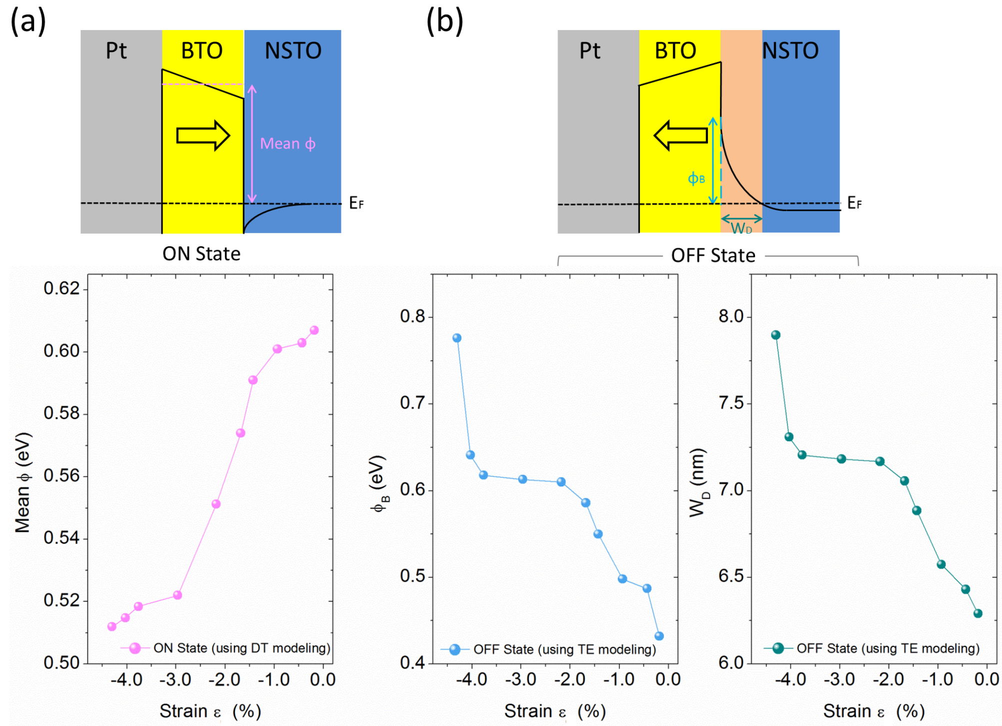

FIG. 5. Schematic illustration of the energy barrier diagram with modeling of barrier profiles for the ON and OFF state with different in-plane strains. Schematic drawings of the MFS-FTJ and (a) corresponding calculated potential energy profiles with mean barrier height for the ON state, and (b) potential barrier height and width of the depletion region of the OFF state as a function of strain obtained by modeling. In the BTO barrier, the arrows denote the polarization directions.

shifts more significantly to a higher value, which shows a similar enhancement of ratio when more compressive strain is added. In order to clarify the mechanism, the graph of conductance against voltage at low bias in the ON state shows the direct tunneling mechanism according to Brinkman [38] (Supplemental, Fig. S4 [36]). For the OFF state, the I-V curves can be fitted by the thermionic emission model as shown in Fig. 4(b).

A roughly parabolic dependence of conductance on voltage suggests a trapezoidal barrier with mean barrier height of the 4-u.c.-thick BTO at room temperature as shown in Fig. 5(a). Barrier height increases with decreasing compressive strains, suggesting the probability for tunneling transmittance decreases when strain diminishes and tetragonality decreases. Meanwhile in the OFF state, tunneling model is not suitable; we therefore assume the MFS structure to be a metal-insulator-semiconductor (MIS) structure. The forward bias currents are hence described by the theory of thermionic emission (TE) as the following equation:

$$I_{\text{forward}} = SA^*T^2 \exp\left(-\frac{\varepsilon\varphi_B}{kT}\right)\left[\exp\left(\frac{qV}{nk_BT}\right) - 1\right], \quad (1)$$

where S is the junction area, A^* the Richardson constant, T the absolute temperature, q the electron charge, k the Boltzmann constant, n the ideal factor, and φ_B the Schottky barrier height. From the linear relationship in TE modeling, we can identify the barrier height. The corresponding width of the depletion region, where electrons are depleted at the semiconductor surface when polarization is pointing to metal, can be estimated by Eq. (2):

$$W_D = \left[\frac{2\varepsilon_s}{qN_D}(V_{bi}\text{-}V)\right]^{\frac{1}{2}}, \quad (2)$$

where W_D is the depletion region width, ε_s the dielectric constant of NSTO, N_D the donor concentration [39], $V_{bi} = \varphi_B + \varphi_n$, and $\varphi_n = E_F\text{-}E_c = 0.19\text{eV}$, as reported previously [40]. It is found in Fig. 5(b) that the Schottky barrier becomes wider and higher with increasing compressive strain, resulting in the decrease in junction current. In contrast to the OFF state, the lower the mean barrier, the higher the tunneling transmittance probability at the ON state. This analytical result fits the experimental result of resistance change, as shown in Fig. 3.

IV. DISCUSSION

In this work, with an external in-plane strain adding to the lattice-mismatch-induced strain, the total strain of BTO experiences a large range of strain from $\varepsilon = -0.18\%$ to -4.30% (and can even turn from compressive to tensile strain and results in in-plane polarization if the sample can sustain further bending). Under these strains, as plotted in Fig. 6, the ON/OFF ratio shows a proportional relationship that increases with increasing compressive strain. The ratio can be reversibly tuned with strain, as shown in the Supplemental Fig. S5 [36]. We argue that the origin of this great enhancement is based on a purely mechanical approach, but because of neither the oxygen vacancy movement nor the interfacial electrochemical effect [5,41,42]. As mentioned earlier, in the heterostructured

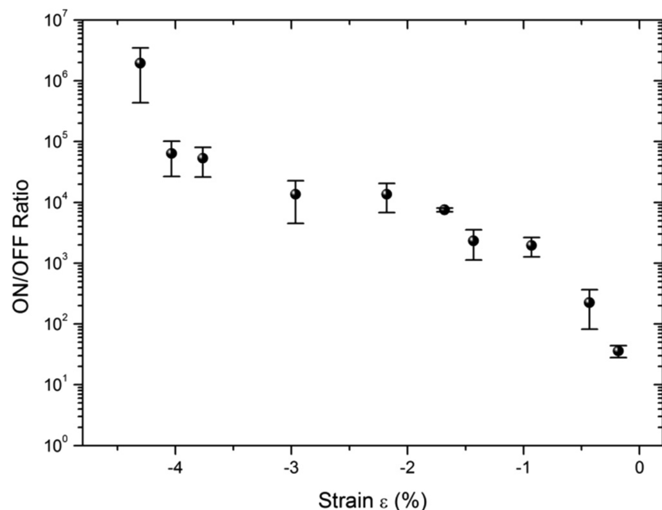

FIG. 6. The ON/OFF ratios as a function of strain, showing the relationship in the ON/OFF ratio in MFS-FTJ for polarization switching as a function of in-plane compressive strain in BTO ultrathin films.

FTJ, these effects are regarded as the reason for the different electroresistance. In other words, not only strains, but plenty of factors are also required to clarify [10,33,42,43]. However, by carrying out the identical electrical measurement to the same tunnel junction in different strain states in our case, the contribution to the electroresistance effect from other factors such as oxygen vacancy movement [25,44] and electrode effect [42] should be almost identical. Therefore, the influence of the change of ferroelectric polarization to the electroresistance of the tunnel junction, which is raised by the change of strain only, can be demonstrated. Moreover, it suggests the Curie temperature (Tc) is also tuned with the change of strain according to Choi [16]. To explain the relationship between Tc and strain, both are factors that will directly induce the change in structure, especially Ti atomic displacement, which originates ferroelectricity. Therefore, Tc can be varied by strain. In particular, for the observed electroresistance changes in FTJ, it is directly related to the spontaneous polarization in ferroelectric materials, and we show that electroresistance changes are varied by strain. Consequently, it is possible to say a tunable Curie temperature can explain the observed electroresistance changes. To simplify, a change in BTO structure (spontaneous polarization) would cause the observed change in electroresistance.

Nevertheless, it should be noticed that flexoelectricity may be considered if the bending angle is large enough. When the bending angle reaches a certain value, polarization induced by the strain gradient would present. As a result, we have to take the net polarization, including ferroelectric and flexoelectric into account [45,46]. In our case, there is a steep change in both depletion width and barrier in the OFF state when $\varepsilon > -3.50\%$. We suggest the flexoelectricity is induced and the net polarization increases in the OFF state. Therefore, the resistance change would be enlarged by this effect. It is not obvious to note the resistance change in the ON state, but the ON/OFF ratio is still enhanced, as when the OFF state resistance dominates the ratio is MIS-FTJ. When ε is smaller than -3.50%, we believe the great enhancement of electroresistance is still based on a pure strain effect.

V. CONCLUSION

In conclusion, dynamic strain engineering in the Pt/BTO/NSTO FTJ has been studied. With an extra compressive strain induced by mechanical stress which is dynamically applied beyond the lattice mismatch, the ON/OFF ratio increases significantly from 10^4 to 10^7, while a mechanical erasing effect can be achieved when a tensile stress is applied. This result shows an advance in the mechanism of tunneling electroresistance as a nonvolatile resistive memory within a simple structure that may avoid factors such as the movement of oxygen vacancies and the interfacial effect on ferroelectric polarization in the resistive switching. Another merit of this external strain engineering is that it provides another way to enhance the ON/OFF ratio and diminish in the memory states through a dynamic mechanical approach.

ACKNOWLEDGMENTS

This work was supported by the financial support of Hong Kong RGC (Grant No. PolyU15309416) and the PolyU Strategic Importance Project (Grants No. 1-ZE25 and No. 1-BBAF). Z.W. acknowledges financial support of the Natural Science Foundation of China (Grant No. 11574169) and the Hong Kong Scholars Program (Grant No. XJ2015024). Experiments were carried out in part at the University Research Facility in Materials Characterization and Device Fabrication, The Hong Kong Polytechnic University.

[1] F. Pan, C. Chen, Z. Wang, Y. Yang, J. Yang, and F. Zeng, Prog. Nat. Sci.: Mater. Int. **20**, 1 (2010).

[2] D. S. Jeong, R. Thomas, R. S. Katiyar, J. F. Scott, H. Kohlstedt, A. Petraru, and C. S. Hwang, Rep. Prog. Phys. **75**, 76502 (2012).

[3] Y. Yang, P. Gao, S. Gaba, T. Chang, X. Pan, and W. Lu, Nat. Commun. **3**, 732 (2012).

[4] Q. Liu, J. Sun, H. Lv, S. Long, K. Yin, N. Wan, Y. Li, L. Sun, and M. Liu, Adv. Mater. **24**, 1774 (2012).

[5] Y. Yang, W. Lü, Y. Yao, J. Sun, C. Gu, L. Gu, Y. Wang, X. Duan, and R. Yu, Sci. Rep. **4**, 3890 (2014).

[6] V. Garcia, S. Fusil, K. Bouzehouane, S. Enouz-Vedrenne, N. D. Mathur, A. Barthélémy, and M. Bibes, Nature (London) **460**, 81 (2009).

[7] A. Chanthbouala *et al.*, Nat. Nanotechnol. **7**, 101 (2012).

[8] A. Gruverman *et al.*, Nano Lett. **9**, 3539 (2009).

[9] V. Garcia and M. Bibes, Nat. Commun. **5**, 4289 (2014).

[10] Z. Wen, C. Li, D. Wu, A. Li, and N. Ming, Nat. Mater. **12**, 617 (2013).

[11] D. J. Kim, H. Lu, S. Ryu, S. Lee, C. W. Bark, C. B. Eom, and A. Gruverman, Appl. Phys. Lett. **103**, 142908 (2013).

[12] C. H. Ahn, Science **303**, 488 (2004).

[13] Y. Wang, W. Chen, B. Wang, and Y. Zheng, Materials (Basel) **7**, 6377 (2014).
[14] E. Y. Tsymbal and H. Kohlstedt, Science **313**, 181 (2006).
[15] M. Y. Zhuravlev, R. F. Sabirianov, S. S. Jaswal, and E. Y. Tsymbal, Phys. Rev. Lett. **94**, 246802 (2005).
[16] K. J. Choi, Science **306**, 1005 (2004).
[17] S. Choudhury, Y. L. Li, L. Q. Chen, and Q. X. Jia, Appl. Phys. Lett. **92**, 142907 (2008).
[18] Y. L. Li and L. Q. Chen, Appl. Phys. Lett. **88**, 072905 (2006).
[19] R. E. Cohen, Nature (London) **358**, 136 (1992).
[20] J. Neaton, C. Hsueh, and K. Rabe, MRS Proceedings **718**, D10. 26 (2002).
[21] D. G. Schlom, L. Q. Chen, C. B. Eom, K. M. Rabe, S. K. Streiffer, and J. M. Triscone, Annu. Rev. Mater. Res. **37**, 589 (2007).
[22] Y. S. Kim *et al.*, Appl. Phys. Lett. **608**, 1 (2005).
[23] D. J. Kim, J. Y. Jo, Y. S. Kim, Y. J. Chang, J. S. Lee, J. G. Yoon, T. K. Song, and T. W. Noh, Phys. Rev. Lett. **95**, 237602 (2005).
[24] V. Nagarajan *et al.*, J. Appl. Phys. **100**, 051609 (2006).
[25] M. Li, J. Li, L.-Q. Chen, B.-L. Gu, and W. Duan, Phys. Rev. B **92**, 115435 (2015).
[26] G. De Luca, M. D. Rossell, J. Schaab, N. Viart, M. Fiebig, and M. Trassin, Adv. Mater. **29**, 1605145 (2016).
[27] E. J. Guo, R. Roth, A. Herklotz, D. Hesse, and K. Dörr, Adv. Mater. **27**, 1615 (2015).
[28] Z. Wen, X. Qiu, C. Li, C. Zheng, X. Ge, A. Li, and D. Wu, Appl. Phys. Lett. **104**, 042907 (2014).
[29] M. D. Biegalski, K. Dörr, D. H. Kim, and H. M. Christen, Appl. Phys. Lett. **96**, 151905 (2010).
[30] Z. Xi, J. Ruan, C. Li, C. Zheng, Z. Wen, J. Dai, A. Li, and D. Wu, Nat. Commun. **8**, 15217 (2017).
[31] T. Shimizu, D. Suwama, H. Taniguchi, T. Taniyama, and M. Itoh, J. Phys.: Condens. Matter **25**, 132001 (2013).
[32] C. L. Jia, V. Nagarajan, J.-Q. He, L. Houben, T. Zhao, R. Ramesh, K. Urban, and R. Waser, Nat. Mater. **6**, 64 (2007).
[33] A. Chanthbouala *et al.*, Nat. Mater. **11**, 860 (2012).
[34] E. Strelcov, Y. Kim, J. C. Yang, Y. H. Chu, P. Yu, X. Lu, S. Jesse, and S. V. Kalinin, Appl. Phys. Lett. **101**, 192902 (2012).
[35] W. Ma and L. E. Cross, Appl. Phys. Lett. **82**, 3293 (2003).
[36] See Supplemental Material at http://link.aps.org/supplemental/10.1103/PhysRevB.95.214304 for structural analysis of junctions and the corresponding performance tests through strain modulation.
[37] H. M. Yau, Z. B. Yan, N. Y. Chan, K. Au, C. M. Wong, C. W. Leung, F. Y. Zhang, X. S. Gao, and J. Y. Dai, Sci. Rep. **5**, 12826 (2015).
[38] W. F. Brinkman, J. Appl. Phys. **41**, 1915 (1970).
[39] K. G. Rana, V. Khikhlovskyi, and T. Banerjee, Appl. Phys. Lett. **100**, 213502 (2012).
[40] Z. Sroubek, Phys. Rev. B **2**, 3170 (1970).
[41] D. J. Kim, H. Lu, S. Ryu, C.-W. Bark, C.-B. Eom, E. Y. Tsymbal, and A. Gruverman, Nano Lett. **12**, 5697 (2012).
[42] R. Soni, A. Petraru, P. Meuffels, O. Vavra, M. Ziegler, S. K. Kim, D. S. Jeong, N. A. Pertsev, and H. Kohlstedt, Nat. Commun. **5**, 5414 (2014).
[43] C. Li *et al.*, Nano Lett. **15**, 2568 (2015).
[44] U. Aschauer, R. Pfenninger, S. M. Selbach, T. Grande, and N. A. Spaldin, Phys. Rev. B **88**, 054111 (2013).
[45] W. Ma and L. E. Cross, Appl. Phys. Lett. **88**, 232902 (2006).
[46] W. Ma, Phys. Scr. **T129**, 180 (2007).